$Tb_2(bpdc)_3$ and $Eu_2(bpdc)_3$ Nanoparticles (bpdc: 2,2′-Bipyridine-4,4′-dicarboxylate) and Their Luminescence

Ana Kuzmanoski and Claus Feldmann
Institut für Anorganische Chemie, Karlsruhe Institute of Technology (KIT), Engesserstraße 15, D-76131 Karlsruhe, Germany

Reprint requests to Prof. Dr. C. Feldmann. Tel.: ++49-721-60842855.
E-mail: claus.feldmann@kit.edu

Z. Naturforsch. **2014**, *69b*, 248 – 254 / DOI: 10.5560/ZNB.2014-3293
Received October 29, 2013

$Tb_2(bpdc)_3$ and $Eu_2(bpdc)_3$ nanoparticles (bpdc: 2,2′-bipyridine-4,4′-dicarboxylate) have been prepared *via* straightforward precipitation from aqueous solution. The nanoparticles exhibit mean diameters of 41(5) nm ($Tb_2(bpdc)_3$) and 56(4) nm ($Eu_2(bpdc)_3$) and show a very good colloidal stability in aqueous suspension. Particle size and chemical composition have been characterized based on electron microscopy, X-ray diffraction, infrared spectroscopy and thermogravimetry. Photoluminescence validates an efficient excitation of Tb^{3+}/Eu^{3+} *via* the bpdc ligand as an antenna that leads to intense characteristic green and red emissions. The absolute quantum yields of $Tb_2(bpdc)_3$ and $Eu_2(bpdc)_3$ have been determined at 28 and 12 %, respectively. Although rare-earth metal-based photoluminescence is typically quenched in water due to vibronic loss processes (ν(O–H)), here, the antenna effect and the shielding of the metal centers *via* the bpdc ligand are very efficient, allowing for an intense green and red emission of the $Tb_2(bpdc)_3$ and $Eu_2(bpdc)_3$ nanoparticles even in aqueous suspension.

Key words: Terbium, Europium, 2,2′-Bipyridine-4,4′-dicarboxylate, Nanoparticle, Luminescence, Quantum Yield

Introduction

2,2′-Bipyridine-4,4′-dicarboxylic acid (H_2bpdc) and its derivatives belong to the most prominent ligands that can be used for achieving the so-called antenna effect [1]. The ligand guarantees for an efficient light absorption, and the absorbed energy is efficiently transferred to a certain cation. On the one hand, this principle is used in dye-sensitized solar cells (so-called Grätzel cells) for efficient light absorption and fast separation of the generated charge carriers [2, 3]. On the other hand, the antenna effect is widely used for energy transfer to a cation showing intense light emission [4]. This strategy is very powerful in order to populate high-energy levels of trivalent rare-earth ions, such as Tb^{3+} or Eu^{3+}. For them, a direct excitation into the *f*-manifold *via* light absorption is spin and/or parity forbidden [5]. As a consequence, the *f*-lines of the rare-earth ions show only minor absorption strength – and thus, a weak absorption and emission. For molecular complexes of Tb^{3+} or Eu^{3+} with the bpdc ligand the energy transfer is known to be very efficient. Even when dissolved in water, or with water coordinated directly to the rare-earth metal center, the luminescence is not quenched by the O–H vibration [6 – 8].

While luminescent molecular complexes as well as bulk metalorganic frameworks of rare-earth cations and the bpdc ligand have been widely investigated (bpdc: 2,2′-bipyridine-4,4′-dicarboxylate) [9 – 12], rare-earth metal 2,2′-bipyridine-4,4′-dicarboxylates as nanoparticles have not been reported till now. The advantage of such nanoparticles is related, on the one hand, to the quasi infinite number of luminescent centers in a single nanoparticle that allows for a much higher emission intensity as compared to the limited number of luminescent centers in a molecular complex. On the other hand, the differentiation between a luminescent nanoparticle and the non-luminescent solvent – thus, the contrast between light and dark – is much higher as compared to a homogeneous solution of luminescent molecular complexes. Both these

aspects are highly relevant for the application of luminescent nanoparticles in terms of labeling, advertising, security markers, or optical imaging [13, 14].

Here, we report on the synthesis of $Tb_2(bpdc)_3$ and $Eu_2(bpdc)_3$ nanoparticles. These nanoparticles exhibit a very good dispersibility in water and show an efficient excitation of Tb^{3+}/Eu^{3+} *via* the antenna effect of the bpdc ligand, followed by intense green and red light emission. Since the nanoparticles contain molar quantities of the rare-earth cation (thus, it is not a doping) and of the bpdc ligand (thus, it is not a surface capping), the absorption and emission intensity per nanoparticle is very high.

Results and Discussion

The synthesis of $Tb_2(bpdc)_3$ and $Eu_2(bpdc)_3$ nanoparticles was performed *via* straightforward precipitation from aqueous solution. To this end, the rare earth chlorides were dissolved in water and injected at 60 °C into an aqueous solution of H_2bpdc. The nucleation of the nanoparticles was initiated according to LaMer's model of particle nucleation and growth from homogeneous solution with a supersaturation established after the hot-injection [15]. In addition to the temperature during the injection, two additional aspects have to be considered to obtain nanoparticles. On the one hand, the acidity of the 2,2′-bipyridine-4,4′-dicarboxylic acid needs to be moderated by addition of Na_2CO_3 to a slightly basic pH of 8.5. On the other hand, the bpdc ligand has to be added with a significant molar excess (33 %). As a consequence, excess bpdc is continuously available for surface adsorption during particle growth. Due to its size as well as its charge, the bpdc capping on the surface guarantees for a sufficient steric as well as electrostatic stabilization of the nanoparticles [16]. As a result, the nanoparticle suspensions have a very high colloidal stability and do not show any precipitation on the timescale of several weeks.

The size and shape of the as-prepared $Tb_2(bpdc)_3$ and $Eu_2(bpdc)_3$ nanoparticles were investigated in suspension by dynamic light scattering (DLS), and as a powder by scanning electron microscopy (SEM). DLS analysis of $Tb_2(bpdc)_3$ in water shows a comparably narrow size distribution with a mean hydrodynamic diameter of 41(5) nm (Fig. 1). The hydrodynamic diameter of the Eu^{3+} particles is somewhat larger and at a mean value of 56(4) nm (Fig. 1). According to SEM, $Tb_2(bpdc)_3$ and $Eu_2(bpdc)_3$ particles exhibit a spherical shape and a high uniformity. The mean particle diameter was determined based on a statistical evaluation of at least 100 nanoparticles and resulted in 20(5) nm for $Tb_2(bpdc)_3$ and 40(5) nm for $Eu_2(bpdc)_3$. Thus, the particle diameter as determined from SEM is below the hydrodynamic diameter stemming from DLS. This finding is in accordance with expectation since the non-mobile solvent shell surrounding the nanoparticles is comparably thick for water as a highly polar solvent. Moreover, some agglomeration occurs in aqueous suspension. Considering the fact that the nanoparticles were obtained *via* simple precipitation from aqueous solution without any specific colloidal stabilizer involved, the particle size and size distribution of the as-prepared $Tb_2(bpdc)_3$ and $Eu_2(bpdc)_3$ are indicative of a high quality.

To identify the chemical composition of the as-prepared nanoparticles, powder X-ray diffraction (XRD) analysis, Fourier-transform infrared spectroscopy (FT-IR) and thermogravimetry (TG) were conducted. According to XRD, however, the nanoparticles turned out to be completely amorphous and do not show specific Bragg peaks. The FT-IR spectra of the nanoparticles were compared to that of 2,2′-bipyridine-4,4′-dicarboxylic acid as a free ligand (Fig. 2). While the characteristic molecular vibrations are clearly visible (ν(C–H): 2950 – 2800 cm^{-1}, ν_{as}(OCO): 1750 – 1700 cm^{-1}, ν_s(OCO): 1300 – 1250 cm^{-1}, fingerprint area: 1250 – 600 cm^{-1}), significant differences between the nanoparticles and the free ligand become obvious. While the wavenumber of ν_{as}(OCO) is decreased to 1650 – 1600 cm^{-1}, ν_s(OCO) is increased to 1450 – 1400 cm^{-1}. This finding can be rationalized based on a bpdc ligand that is deprotonated and coordinated as a chelate to a metal center in the nanoparticle. Moreover, the manifold of sharp bands referring to the fingerprint area (1250 – 600 cm^{-1}) is only of minor intensity for the nanoparticles. This is due to the low site symmetry of the ligands in the amorphous, solid nanoparticles. Together, these data provide good evidence that Tb^{3+}/Eu^{3+} are coordinated to the carboxylic oxygen atoms of the bpdc ligand, which is also well in accordance with the literature [10]. The broad ν(O–H) vibration at 3700 – 3100 cm^{-1}, moreover, points to a significant absorption of water on the nanoparticle surface. In sum, FT-IR spectra confirm the presence of bpdc in the

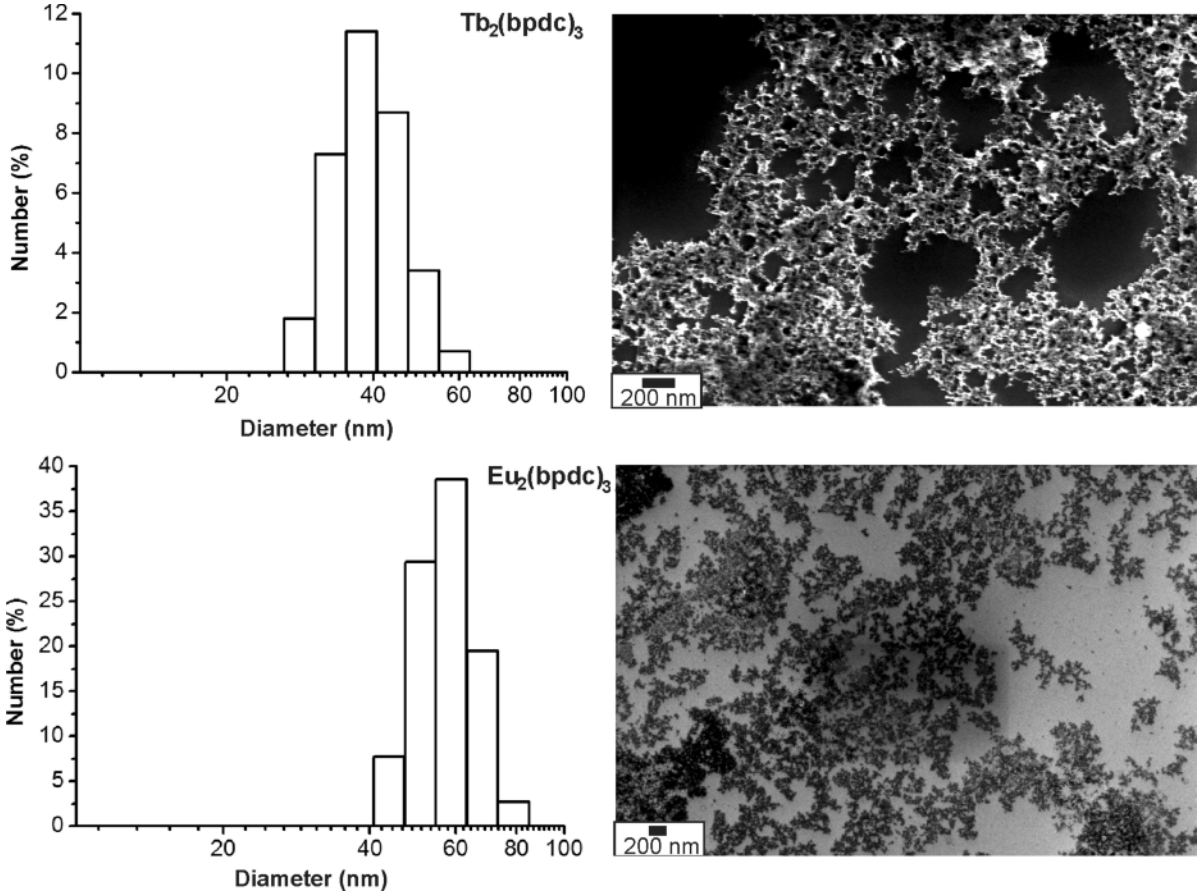

Fig. 1. Particle size and particle size distribution of the as-prepared $Tb_2(bpdc)_3$ and $Eu_2(bpdc)_3$ nanoparticles according to DLS (aqueous suspensions) and SEM analysis.

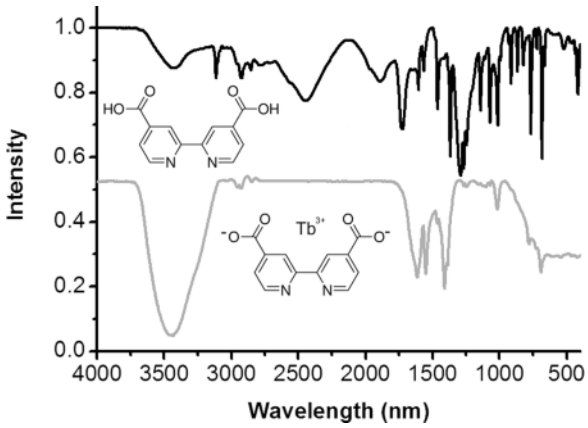

Fig. 2. FT-IR spectra of the as-prepared $Tb_2(bpdc)_3$ nanoparticles and 2,2′-bipyridine-4,4′-dicarboxylic acid (H_2bpdc) shown for comparison.

$Tb_2(bpdc)_3$ and $Eu_2(bpdc)_3$ nanoparticles and indicate its coordination to the metal cation.

In order to confirm the chemical composition of $Tb_2(bpdc)_3$ and $Eu_2(bpdc)_3$ as well as a cation-to-anion ratio of 2 : 3, TG analysis was performed in air (Fig. 3). In order to remove water adsorbed on the particle surface, both materials were first dried in vacuum for 6 h at 50 °C. Thereafter, the powder samples were subjected to TG analysis in air. During heating, both nanoparticle compounds first show a slow weight loss ($Tb_2(bpdc)_3$: 10 wt-% up to 350 °C; $Eu_2(bpdc)_3$: 13 wt-% up to 250 °C) that can be ascribed to a decarboxylation of one of the two carboxylate groups per bpdc molecule (calcd. 12 wt-%). In comparison to bulk materials of similar composition [11], this decarboxylation occurs at reduced temperature, which can be ascribed to the generally higher reactivity of

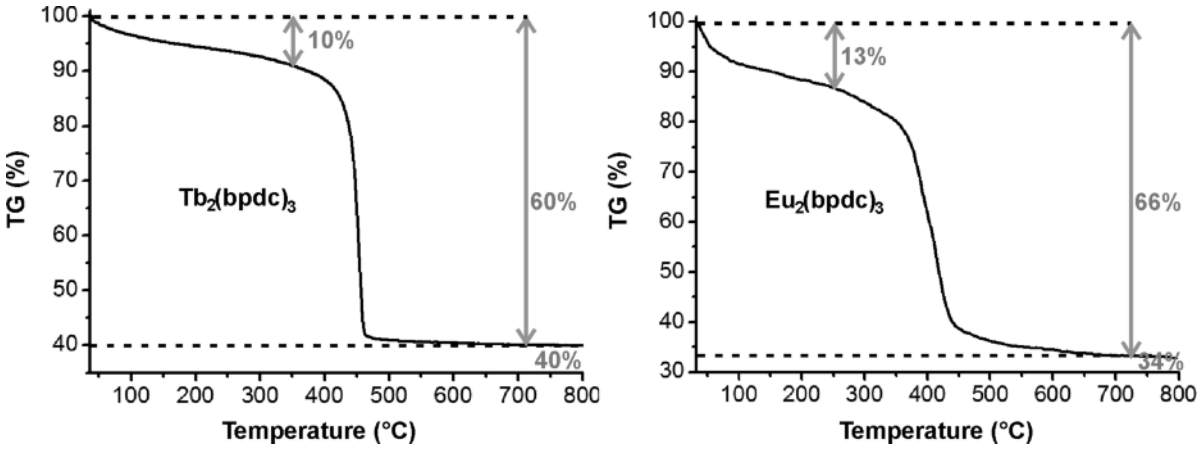

Fig. 3. TGA analysis of the as-prepared $Tb_2(bpdc)_3$ and $Eu_2(bpdc)_3$ nanoparticles (total weight of 10 mg per sample in air).

the nanoparticles. Very strong weight losses of 50 wt-% ($Tb_2(bpdc)_3$) and 53 wt-% ($Eu_2(bpdc)_3$) are observed at 400 – 500 °C ($Tb_2(bpdc)_3$) and 350 – 450 °C ($Eu_2(bpdc)_3$) that are related to a complete oxidative decomposition of the bpdc ligand. The thermal remnants were observed with 40 wt-% ($Tb_2(bpdc)_3$) and 34 wt-% ($Eu_2(bpdc)_3$) and can be identified *via* XRD as Tb_4O_7 and Eu_2O_3. These data can be explained based on the following decomposition processes and calculated weight losses:

(1) $2\,Tb_2(C_{12}H_6N_2O_4)_3 + 72.5\,O_2 \rightarrow$
$72\,CO_2 + 18\,H_2O + 6\,N_2 + Tb_4O_7$
(calcd. 64 %) (calcd. 36 %)

(2) $Eu_2(C_{12}H_6N_2O_4)_3 + 36\,O_2 \rightarrow$
$36\,CO_2 + 9\,H_2O + 3\,N_2 + Eu_2O_3$
(calcd. 66 %) (calcd. 34 %)

Altogether, a total weight loss of 60 wt-% ($Tb_2(bpdc)_3$) and 66 wt-% ($Eu_2(bpdc)_3$) due to the gaseous oxidation products CO_2, H_2O and N_2, as well as the weight of the solid remnant (40 wt-% of Tb_4O_7, 34 wt-% of Eu_2O_3) match well with the calculated data. Thus, a cation-to-anion ratio of 2 : 3 and an overall composition $Tb_2(bpdc)_3$ and $Eu_2(bpdc)_3$ is validated and matches with the bulk composition of already known metalorganic frameworks [9 – 11].

Photoluminescence spectroscopy was used to elucidate the luminescence properties of the as-prepared $Tb_2(bpdc)_3$ and $Eu_2(bpdc)_3$ nanoparticles (Figs. 4 and 5). Both compounds show a broad and intense absorption at 250 to 350 nm indicating the excitation of the bpdc ligand [17]. Notably, excitations *via* the *f*-states of Tb^{3+} and Eu^{3+} are only visible as very weak lines. Emission spectra show an opposite situation as compared to excitation (Figs. 4 and 5). Here, the as-prepared $Tb_2(bpdc)_3$, and $Eu_2(bpdc)_3$ nanoparticles show the characteristic $f \rightarrow f$ emission lines of Tb^{3+} and Eu^{3+} with high intensity [17, 18]. $^5D_4 \rightarrow {}^7F_j$ with $j = 5$ at 544 nm is observed as the dominating emission line for $Tb_2(bpdc)_3$, and $^5D_0 \rightarrow {}^7F_j$ with $j = 2$ at 614 nm for $Eu_2(bpdc)_3$. An emission of the bpdc ligand is, however, not observed. Thus, bpdc serves as an efficient antenna with all the absorbed energy being transferred to the rare-earth centers. The absolute quantum yields of $Tb_2(bpdc)_3$ and $Eu_2(bpdc)_3$ were determined for powder samples by photon counting in an integrating sphere (Ulbricht sphere) and are at mean levels of 28 % for $Tb_2(bpdc)_3$ and 12 % for $Eu_2(bpdc)_3$. Considering the fact that rare-earth metal-based photoluminescence is typically quenched under humid conditions due to ν(O–H)-driven vibronic losses [16, 17], the intense emission of the $Tb_2(bpdc)_3$ and $Eu_2(bpdc)_3$ nanoparticles even in aqueous suspension is surprising and can be very interesting for future applications of such nanomaterials.

Conclusions

$Tb_2(bpdc)_3$ and $Eu_2(bpdc)_3$ (bpdc: 2,2′-bipyridine-4,4′-dicarboxylate) are prepared as nanoparticles *via* controlled precipitation from aqueous solution. These suspensions show a high colloidal stability and

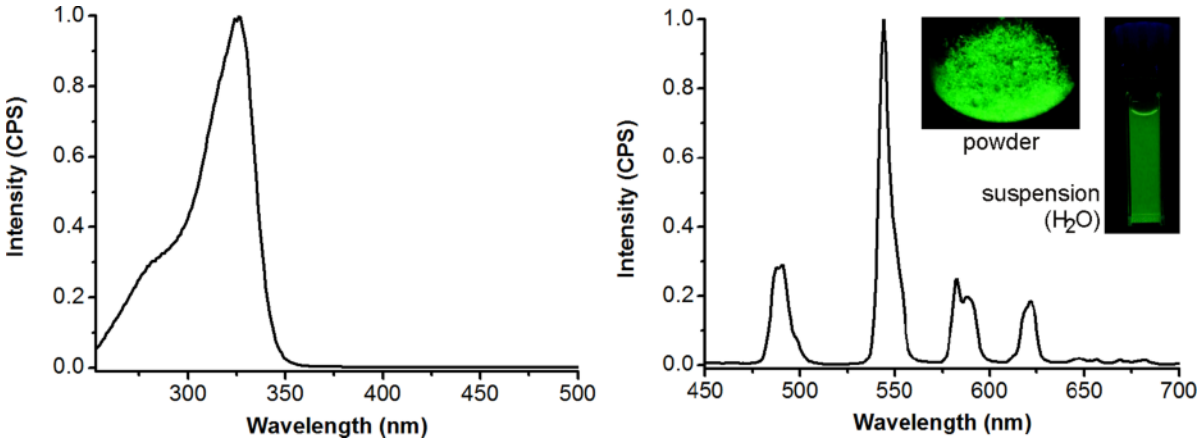

Fig. 4 (color online). Luminescence characterization of the as-prepared $Tb_2(bpdc)_3$ nanoparticles in aqueous suspension: excitation spectrum ($\lambda_{em} = 544$ nm), emission spectrum ($\lambda_{exc} = 326$ nm) and photos showing the emission ($\lambda_{exc} = 366$ nm) of powder and aqueous suspension (all data measured at room temperature).

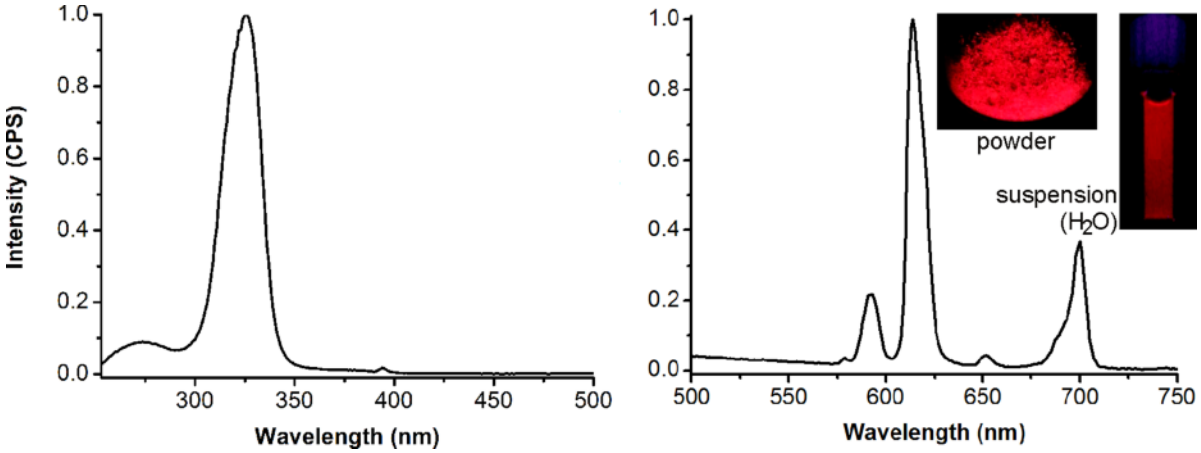

Fig. 5 (color online). Luminescence characterization of the as-prepared $Eu_2(bpdc)_3$ nanoparticles in aqueous suspension: excitation spectrum ($\lambda_{em} = 614$ nm), emission spectrum ($\lambda_{exc} = 343$ nm) and photos showing the emission ($\lambda_{exc} = 366$ nm) of powder and aqueous suspension (all data measured at room temperature).

mean diameters of 41(5) nm for $Tb_2(bpdc)_3$ and of 56(4) nm for $Eu_2(bpdc)_3$. The nanoparticles are non-crystalline, and their chemical composition has been validated based on FT-IR spectroscopy and fluorescence spectroscopy. Thermogravimetry shows the thermal decomposition of the bpdc ligand and formation of Tb_4O_7/Eu_2O_3 as the solid remnants. By quantifying this decomposition, the composition $Tb_2(bpdc)_3/Eu_2(bpdc)_3$ and the cation-to-anion ratio of 2 : 3 have been confirmed. Luminescence spectra provide evidence for an efficient excitation of Tb^{3+}/Eu^{3+} *via* the antenna effect of the bpdc ligand as well as an intense characteristic green and red emission. Since the nanoparticles contain the rare earth cation and the bpdc ligand in molar quantities, the number of luminescent centers per nanoparticle, and thus the absorption and emission intensity, are very high. Although rare-earth metal-based photoluminescence is typically quenched in water due to relaxation *via* the O–H vibration, the antenna effect and shielding of the metal centers *via* the bpdc ligand is very efficient, allowing for an intense green and red emission of the $Tb_2(bpdc)_3$ and $Eu_2(bpdc)_3$ nanoparticles with quantum yields of 28 and 12 %, respectively. Be-

ing based on a straightforward synthesis and showing an intense green and red emission in water-based suspensions, $Tb_2(bpdc)_3$ and $Eu_2(bpdc)_3$ nanoparticles can become relevant for applications, such as labeling, advertising, security marking, or optical imaging.

Experimental Section

Materials and synthesis

All chemicals were used as received from the supplier: terbium chloride hexahydrate (Aldrich, 99.9 %), europium chloride hexahydrate (Aldrich, 99.9 %), 2,2′-bipyridine-4,4′-dicarboxylic acid (H_2bpdc) (ABCR, 98 %), sodium carbonate (Fluka, 99.9 %). All preparative work could be performed in air. Inert conditions are not necessary which facilitates the synthesis significantly.

The synthesis of the $Tb_2(bpdc)_3$ and $Eu_2(bpdc)_3$ nanoparticles was performed by precipitation from aqueous solution. To this end, 10 mg (0.04 mmol) of H_2bpdc was dissolved in 20 mL degassed demineralized water. By addition of Na_2CO_3, the pH of the acidic solution was increased to about pH = 8.5. The colorless solution was heated to 60 °C. Thereafter, an aqueous solution of 10 mg of the respective rare earth chloride (0.03 mmol) in 2 mL of water was added *via* hot-injection. Particle nucleation started instantaneously and resulted in a colorless suspension. Afterwards, the suspension was heated for 1 h at 60 °C. The resulting nanoparticles were separated by centrifugation and purified by sequential resuspension/centrifugation in/from water. Finally, the nanoparticles were washed once with ethanol. For analytical characterization, the as-prepared colorless $Tb_2(bpdc)_3$ and $Eu_2(bpdc)_3$ nanoparticles were used as aqueous suspensions or as powders.

Analytical techniques

Scanning electron microscopy (SEM) was conducted on a Zeiss Supra 40 VP, using an acceleration voltage of 10 kV and a working distance of 2 mm. As-prepared samples were redispersed in water or ethanol and deposited on silicon wafers as sample holders for SEM investigation.

Dynamic light scattering (DLS) was performed with a Nanosizer ZS from Malvern Instruments. For DLS analysis as-prepared particles were redispersed in water. The nanoparticle diameter was measured in aqueous suspension applying polystyrene cuvettes.

Powder X-ray diffraction (XRD) was conducted with a Stoe STADI-P operating with Ge-monochromatized CuK_α radiation.

Infrared spectra (FT-IR) were measured with a Bruker Vertex 70 FT-IR instrument. The samples were measured in KBr pellets with a resolution of 4 cm^{-1}.

Thermogravimetry (TG) was performed with a Netsch STA 409C analyzer. The samples were heated in air to a maximum temperature of 800 °C with a heating rate of 1 K min^{-1}.

Photoluminescence (PL) was recorded for the powder samples with a Jobin Yvon Spex Fluorolog 3.2 equipped with a 450 W Xe lamp, an integrating sphere as well as double grating excitation and emission monochromators. The absolute quantum yield was determined for powder samples according to Friend [19]. Thus, the diffuse reflection of the sample was first determined at a certain excitation wavelength. Next, the emission was measured under excitation at the same wavelength. Integration over the reflected and emitted photons by use of the Ulbricht sphere resulted in the absolute quantum yield. Corrections were made taking into account the spectral power of the excitation source, the reflection behavior of the Ulbricht sphere, and the sensitivity of the detector.

Acknowledgement

The authors are grateful to the Center for Functional Nanostructures (CFN) of the Deutsche Forschungsgemeinschaft (DFG) at the Karlsruhe Institute of Technology (KIT) for financial support.

[1] J. M. Lehn, *Angew. Chem., Int. Ed. Engl.* **1990**, *29*, 1304.
[2] B. O'Regan, M. Graetzel, *Nature* **1991**, *353*, 737.
[3] X. Chen, C. Li, M. Graetzel, R. Kostecki, S. S. Mao, *Chem. Soc. Rev.* **2012**, *41*, 7909.
[4] J.-C. G. Bünzli, L. J. Charbonnière, R. F. Ziessel, *J. Chem. Soc., Dalton Trans.* **2000**, 1917.
[5] S. Shionoya, W. M. Yen, *Phosphor Handbook*, CRC, Boca Raton **1999**.
[6] K. L. Wong, P. A. Tanner, *Inorg. Chem.* **2007**, *46*, 9754.
[7] J. M. Zhou, W. Shi, N. Xu, P. Cheng, *Inorg. Chem.* **2013**, *52*, 8082.
[8] D. T. Thielemann, A. T. Wagner, E. Birtalan, D. Kölmel, J. Heck, B. Rudat, M. Neumaier, C. Feldmann, U. Schepers, S. Bräse, P. W. Roesky, *J. Am. Chem. Soc.* **2013**, *135*, 7454.
[9] J. W. Dai, M. L. Tong, *Cryst. Eng. Comm.* **2012**, *14*, 2124.

[10] G. L. Law, K. L. Wong, Y. Y. Yang, Q. Y. Yi, G. Jia, W. T. Wong, P. A. Tanner, *Inorg. Chem.* **2007**, *46*, 9754.
[11] J. Y. Wu, T. T. Yeh, Y. S. Wen, J. Twu, K. L. Lu, *Cryst. Growth Design* **2006**, *6*, 467.
[12] P. S. Calefi, A. O. Ribeiro, A. M. Pires, O. A. Serra, *J. Alloys Comp.* **2002**, *344*, 285.
[13] H. Althues, J. Henle, S. Kaskel, *Chem. Soc. Rev.* **2007**, *36*, 1454.
[14] J. G. Fujimoto, D. Farkas, *Biomedical Optical Imaging*, Oxford University Press, Oxford **2009**.
[15] V. K. LaMer, R. H. Dinegar, *J. Am. Chem. Soc.* **1950**, *72*, 4847.
[16] H. Goesmann, C. Feldmann, *Angew. Chem. Int. Ed.* **2010**, *49*, 1362.
[17] G. Blasse, C. Grabmaier, *Luminescent Materials*, Springer, Berlin **1994**.
[18] P. S. Calefi, A. O. Ribeiro, A. M. Pires, O. A. Serra, *J. Alloys Comp.* **2002**, *344*, 285.
[19] J. V. de Mello, H. F. Wittmann, R. H. Friend, *Adv. Mater.* **1997**, *9*, 230.